

VIP

# Improving Photocurrent Generation: Supramolecularly and Covalently Functionalized Single-Wall Carbon Nanotubes–Polymer/Porphyrin Donor–Acceptor Nanohybrids

G. M. Aminur Rahman,<sup>[a]</sup> Anna Troeger,<sup>[a]</sup> Vito Sgobba,<sup>[a]</sup> Dirk M. Guldi,<sup>\*[a]</sup> Norbert Jux,<sup>[b]</sup> Domenico Balbino,<sup>[b]</sup> Maxim N. Tchoul,<sup>[c]</sup> Warren T. Ford,<sup>[c]</sup> Aurelio Mateo-Alonso,<sup>[d]</sup> and Maurizio Prato<sup>\*[d]</sup>

**Abstract:** Novel nanohybrids based on covalently and noncovalently functionalized single-wall carbon nanotubes (SWNTs) have been prepared and assembled for the construction of photoactive electrodes. Polymer-grafted SWNTs were synthesized by free-radical polymerization of (vinylbenzyl)trimethylammonium chloride. Poly[(vinylbenzyl)trimethylammonium chloride] (PVBTA<sup>n+</sup>) was also noncovalently wrapped around SWNTs to form stable, positively charged SWNT/PVBTA<sup>n+</sup> suspensions in water. Versatile donor–acceptor nanohybrids were

prepared by using the electrostatic/van der Waals interactions between covalent SWNT–PVBTA<sup>n+</sup> and/or noncovalent SWNT/PVBTA<sup>n+</sup> and porphyrins (H<sub>2</sub>P<sup>8-</sup> and/or ZnP<sup>8-</sup>). Several spectroscopic, microscopic, transient, and photoelectrochemical measurements were taken to characterize the resulting supramolecular complexes. Photoexcitation of the nanohybrids afforded

long-lived radical ion pairs with lifetimes as long as 2.2 μs. In the final part, photoactive electrodes were constructed by using a layer-by-layer technique on an indium tin oxide covered glass support. Photocurrent measurements gave remarkable internal photon-to-current efficiencies of 3.81 and 9.90% for the covalent ZnP<sup>8-</sup>/SWNT–PVBTA<sup>n+</sup> and noncovalent ZnP<sup>8-</sup>/SWNT/PVBTA<sup>n+</sup> complex, respectively, when a potential of 0.5 V was applied.

**Keywords:** charge transfer • donor–acceptor systems • nanotubes • porphyrinoids • solar cells

[a] Dr. G. M. A. Rahman, A. Troeger, Dr. V. Sgobba, Prof. D. M. Guldi  
Department of Chemistry and Pharmacy &  
Interdisciplinary Center for Molecular Materials  
University of Erlangen-Nürnberg  
Egerlandstrasse 3, 91058 Erlangen (Germany)  
Fax: (+49)913-1852-8307  
E-mail: dirk.guldi@chemie.uni-erlangen.de

[b] Priv.-Doz. Dr. N. Jux, D. Balbino<sup>†</sup>  
Department of Chemistry and Pharmacy &  
Interdisciplinary Center for Molecular Materials  
University of Erlangen-Nuremberg  
Henkestr. 42  
91054 Erlangen (Germany)

[c] Dr. M. N. Tchoul, Prof. W. T. Ford  
Department of Chemistry, Oklahoma State University  
Stillwater, OK 74078 (USA)

[d] Dr. A. Mateo-Alonso, Prof. M. Prato  
Center of Excellence for Nanostructured Materials, CENMAT  
Dipartimento di Scienze Farmaceutiche and INSTM  
University of Trieste  
Piazzale Europa 1, 34127 Trieste (Italy)  
Fax: (+39)040-52572  
E-mail: prato@units.it

[<sup>†</sup>] This author (Domenico Balbino) has been added since the first online publication of this article. The authors sincerely apologize for this oversight; March 3, 2009.

Supporting information for this article is available on the WWW under <http://dx.doi.org/10.1002/chem.200801018>.

## Introduction

Synthetic multifunctional composites are materials designed to combine multiple performance capabilities in a single system. In designing such systems, the correct combination of the individual components plays an enormous role. Therefore, the choice of materials is of fundamental importance. Among the materials currently under consideration for novel photovoltaic devices, single-wall carbon nanotubes (SWNTs) and porphyrins are undergoing careful screening. SWNTs are one of the most striking discoveries in chemistry and materials science due to their outstanding mechanical, electrical, thermal, and optical properties.<sup>[1–3]</sup> They have been investigated for numerous potential applications, for example, molecular electronics,<sup>[4]</sup> nanowires,<sup>[5]</sup> field-effect transistors,<sup>[6]</sup> biochemical sensors,<sup>[7]</sup> and memory elements.<sup>[8]</sup> However, most of these applications can only be realized through the solid-phase deposition of carbon nanotubes at the site of action<sup>[9]</sup> or by in situ growth.<sup>[10]</sup> Strong van der Waals attractions between individual SWNTs causes the formation of dense aggregates, that is, a robust network of

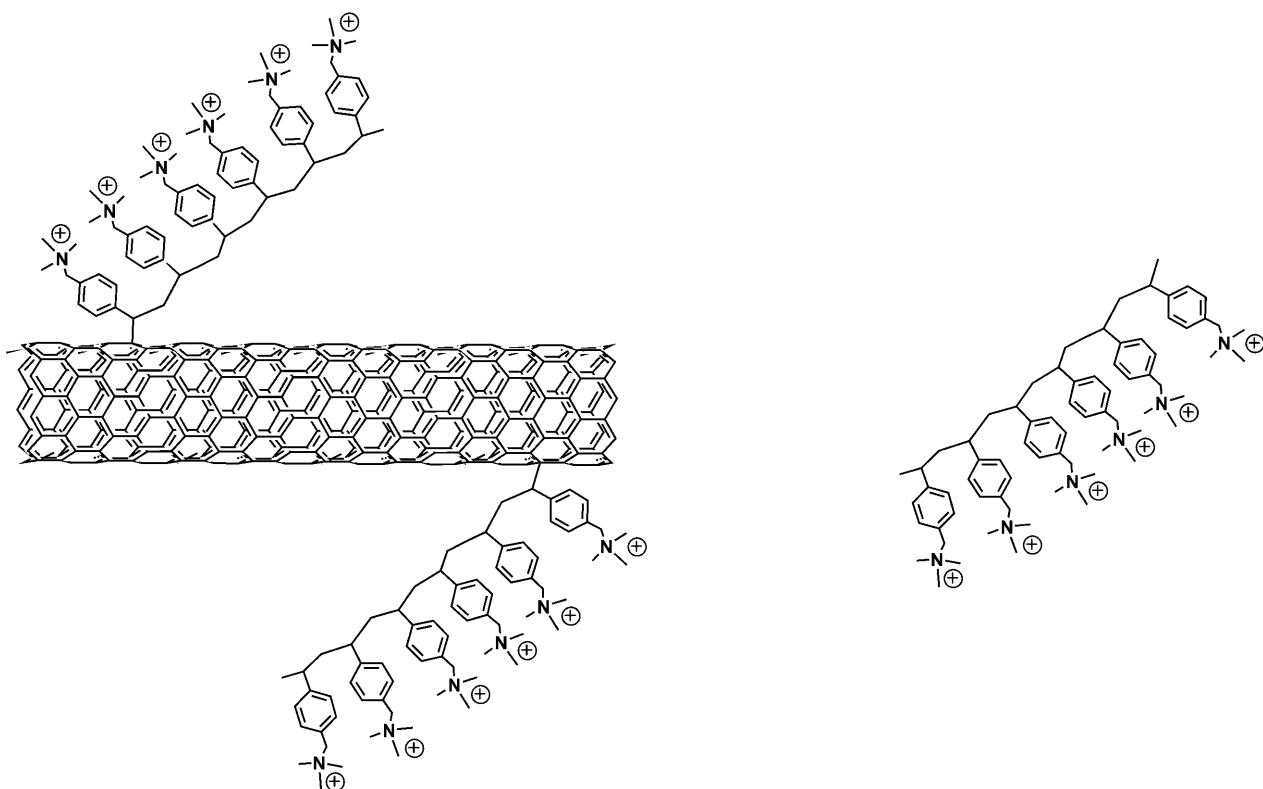
ropes of individual 1 nm diameter SWNTs (usually 10–30 nm in diameter and several  $\mu\text{m}$  in length).

Solution-phase processing of SWNTs is very difficult, especially considering the general insolubility of these materials in most organic and aqueous solvents.<sup>[11]</sup> To fully exploit the potential of SWNTs as integrative building blocks for macroscopic functional devices, critical issues such as limited solubility, dispersibility, and processibility have to be overcome. To this end several approaches have been developed in recent years, which include covalent sidewall functionalizations<sup>[12]</sup> and noncovalent exohedral interactions.<sup>[13]</sup> Covalent functionalization alters or even destroys the electronic and mechanical features of SWNTs. In stark contrast, noncovalent interactions preserve nearly all the intrinsic properties of SWNTs.<sup>[14]</sup> Among these approaches, covalent sidewall modification with polymeric structures has shown great promise for improving the overall solubility of the SWNTs.<sup>[15]</sup> Additionally, through this approach, the electronic properties of SWNTs can be maintained by keeping a low degree of sidewall functionalization because the large size and solubilization power of the polymeric addends overcome the solubility problems (this is in contrast to low-molecular-weight addends that require a higher degree of functionalization to increase solubility). As a matter of fact, polymer-functionalized SWNTs are relatively easy to disperse in organic<sup>[16]</sup> and aqueous<sup>[17]</sup> media. In addition to the solubility properties, SWNT functionalization has also resulted in the preparation of SWNT–polymer hybrids with tailored physicochemical<sup>[18]</sup> and mechanical properties.<sup>[19]</sup>

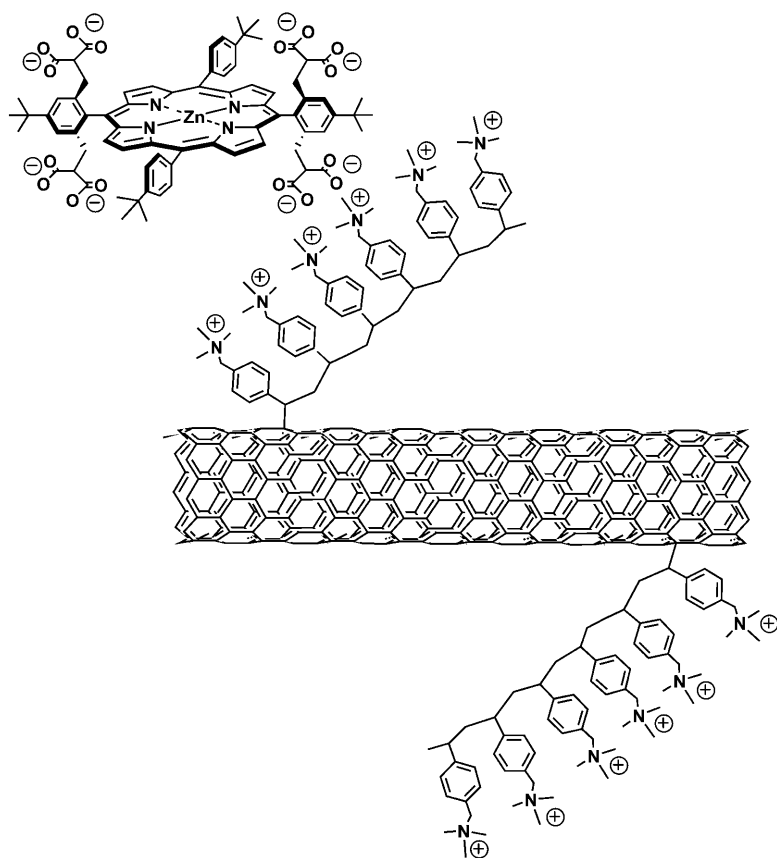
These have been applied in the reinforcement of various polymers.<sup>[20]</sup>

Polymer-functionalized SWNTs are expected to find a prominent position in electro- and photoactive nanocomposites, mainly due to the electron-accepting properties of SWNTs.<sup>[21]</sup> In fact, it has been established that the combination of SWNTs and electron-donor groups is an excellent way to prepare novel materials for applications in solar energy conversion systems.<sup>[22]</sup> Recently the association of covalently and noncovalently linked carbon nanotube (CNT) nanoconjugates with porphyrins afforded CNT-based donor-acceptor nano hybrids, which, upon illumination with visible light, give rise to the formation of long-lived charge-separated species.<sup>[23,24]</sup> The lifetimes of the charge-separated states are so long that these systems have been used with great success for the fabrication of photovoltaic devices.<sup>[25]</sup>

SWNTs can be covalently grafted with water-soluble poly-[(vinylbenzyl)trimethylammonium chloride] (PVBTA<sup>n+</sup>) by the free-radical polymerization of the monomer in the presence of SWNTs (see Scheme 1), which produces material that is 62:38 SWNT/PVBTA<sup>n+</sup> by weight and almost maintains the inherent properties of the SWNTs.<sup>[26]</sup> The presence of the positively charged polymer increased enormously the solubility in water. Indeed, the resulting aqueous dispersions are stable for months without showing any appreciable precipitation. According to atomic force microscopy (AFM) observations, the aqueous suspensions consist principally of individual and/or small bundles of SWNTs. An advantage of SWNT–PVBTA<sup>n+</sup> is the presence of positive charges on the



Scheme 1. Structures of SWNT–PVBTA<sup>n+</sup> (left) and PVBTA<sup>n+</sup> (right).



Scheme 2. Partial structure of covalent SWNT-PVBTA<sup>n+</sup>/ZnP<sup>8-</sup> nanohybrids.

grafted polymer, which allows functionalization through electrostatic interactions with negatively charged species (see Scheme 2).

In this paper we report on the advantages, in terms of solar energy conversion in solution and at photoelectrodes, that emerge from coulombic complexes formed between polyanionic porphyrin derivatives and covalent SWNT-PVBTA<sup>n+</sup> and/or the noncovalent SWNT/PVBTA<sup>n+</sup> complexes. Very long lifetimes of the radical ion pair accompany a remarkable photoperformance. In particular, monochromatic incident photon-to-current conversion efficiency (IPCE) values of up to 9.90% for a single sandwich layer of SWNT/PVBTA<sup>n+</sup> and a zinc porphyrin are the highest values ever reported for comparable systems.

## Results and Discussion

Figures 1 and 6 show that both components, SWNT and PVBTA<sup>n+</sup>, are present in the absorption spectrum of an aqueous solution of covalent SWNT-PVBTA<sup>n+</sup> with features of the polymer in the ultraviolet region and the characteristic van Hove singularities of SWNTs (i.e., transitions in semiconducting and metallic SWNTs) in the visible and near-infrared regions. The presence of the van Hove singularities indicates that a moderate modification of the elec-

tronic structure occurred during the free-radical polymerization.

AFM and transmission electron microscopy (TEM) are powerful tools for determining the distribution of the diameters and lengths of CNTs. A typical AFM image of covalent SWNT-PVBTA<sup>n+</sup> is shown in Figure 2; aggregates and small bundles are discernable, the lengths of which vary between several hundred nanometers and several micrometers. Figure 3 shows a TEM image of bundles of nanotubes, which correlate with the AFM observations.

The absorptions of ZnP<sup>8-</sup> or H<sub>2</sub>P<sup>8-</sup>, namely, strong Soret-type transitions in the 400–450 nm region and weaker Q-type transitions in the 500–650 nm range, were monitored as variable amounts of covalent SWNT-PVBTA<sup>n+</sup> were added (see Figure 4 and Figure S1 in the Supporting Information). Although the porphyrin concentration was kept

constant during these assays noticeable weakening of the Soret- and Q-bands was registered, accompanied by a general broadening of the SWNT absorptions throughout the entire UV/Vis/NIR region. Similarly, the porphyrin-centered absorption bands were redshifted and broadened. Isosbestic points were observed at 429 and 420 nm for ZnP<sup>8-</sup> and H<sub>2</sub>P<sup>8-</sup>, respectively (Figure 4 and Figure S2).

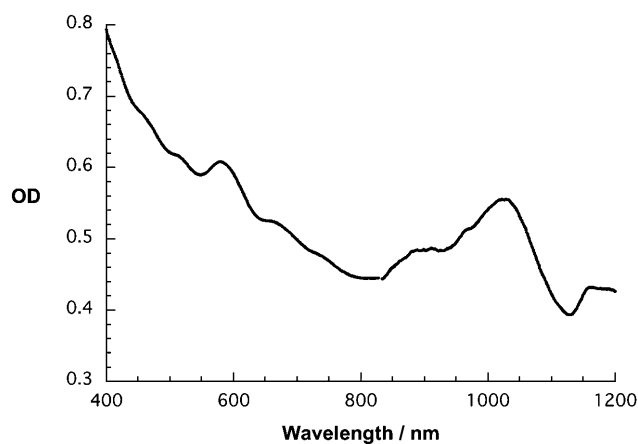


Figure 1. Absorption spectrum of covalent SWNT-PVBTA<sup>n+</sup> in D<sub>2</sub>O at room temperature.

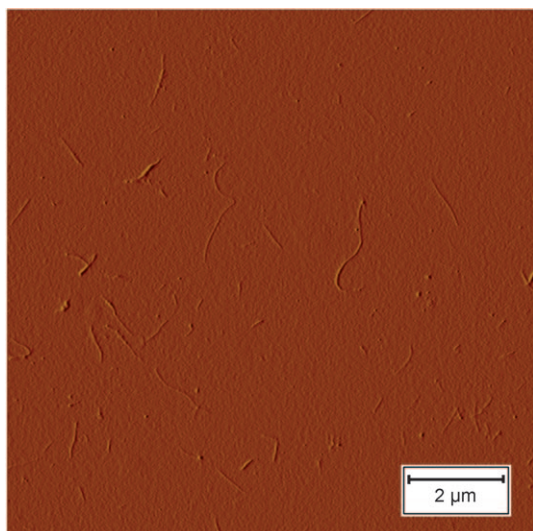


Figure 2. AFM image of covalent SWNT-PVBTA<sup>n+</sup> on a silicon wafer.

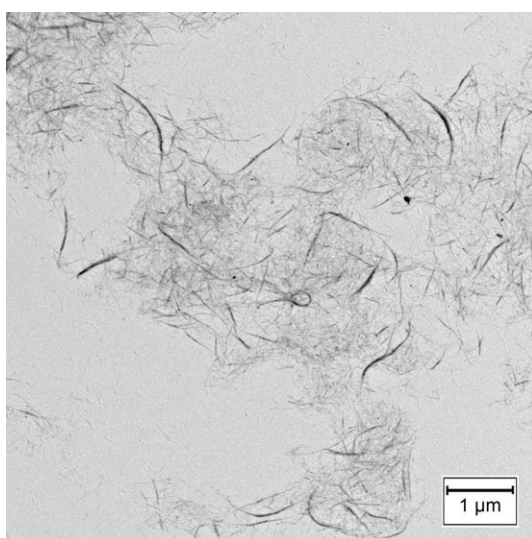


Figure 3. TEM image of covalent SWNT-PVBTA<sup>n+</sup>.

All these pieces of evidence are an indication of a clean adduct-to-product transformation, which, in the current context, points to the immobilization of photoactive ZnP<sup>8-</sup> or H<sub>2</sub>P<sup>8-</sup> on SWNT-PVBTA<sup>n+</sup>. The wavelengths of the isosbestic points were therefore selected to photoexcite the same solutions (i.e., ZnP<sup>8-</sup>/SWNT-PVBTA<sup>n+</sup> or H<sub>2</sub>P<sup>8-</sup>/SWNT-PVBTA<sup>n+</sup>) under steady-state conditions (see Figure 5 and Figure S2 in the Supporting Information).

These fluorescence assays showed a nonlinear, exponential quenching of the ZnP<sup>8-</sup> and H<sub>2</sub>P<sup>8-</sup> fluorescence at 608 and 645 nm, respectively. A quantitative analysis showed that the fluorescence quenching depends exclusively on the concentration of SWNT-PVBTA<sup>n+</sup>. At higher SWNT-PVBTA<sup>n+</sup> concentrations the fluorescence quenching leveled off and converged towards a constant value. At this point, the quenching is quantitative and the immobilization

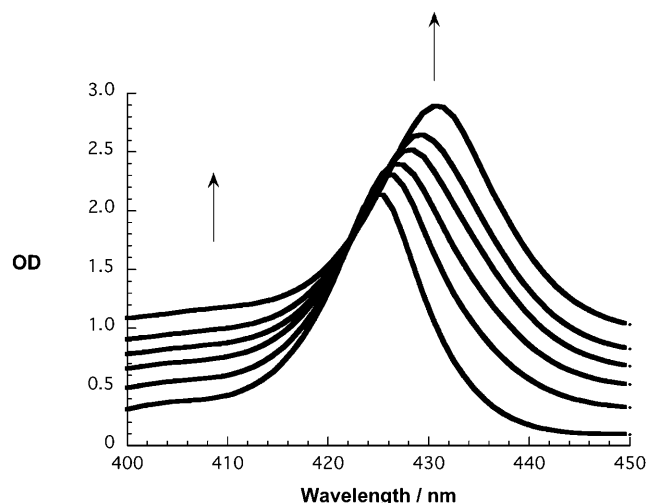


Figure 4. Absorption spectra of a dilute aqueous solution of ZnP<sup>8-</sup> ( $5.0 \times 10^{-6}$  M) with variable concentrations of SWNT-PVBTA<sup>n+</sup>. The arrows indicate the progression.

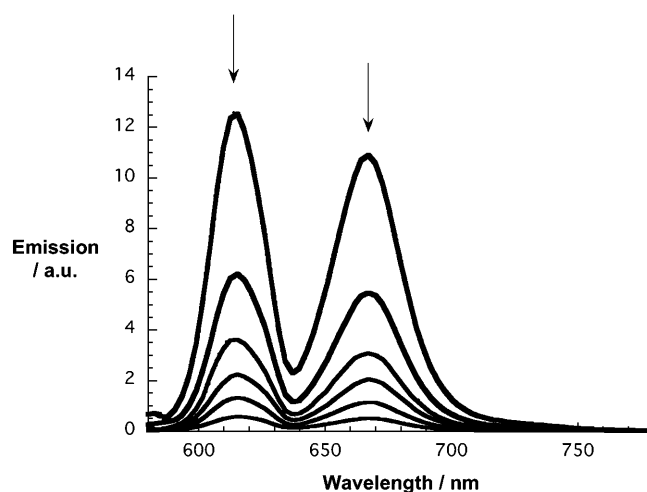
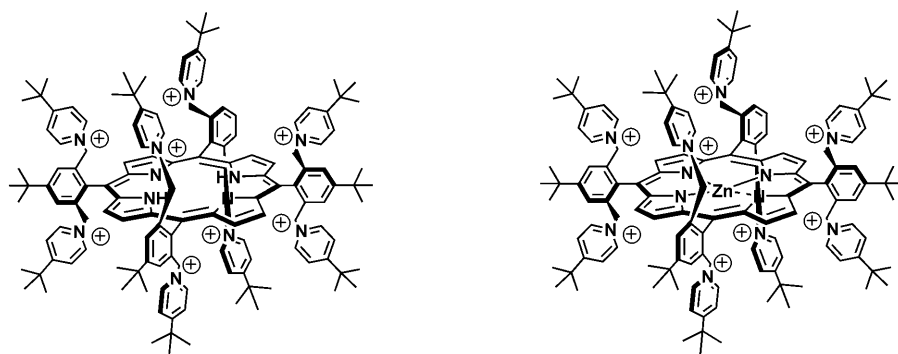


Figure 5. Steady-state fluorescence spectra of a dilute aqueous solution of ZnP<sup>8-</sup> ( $5.0 \times 10^{-6}$  M) with variable concentrations of SWNT-PVBTA<sup>n+</sup> ( $10.6 \text{ mg L}^{-1}$ ). The arrows indicate the progression.

is considered to be complete. Importantly, in the corresponding reference experiments with only PVBTA<sup>n+</sup> (without SWNTs), absorption spectrophotometry confirmed the electrostatically driven binding (Figure S3 in the Supporting Information). The absence of the electron-accepting SWNTs in ZnP<sup>8-</sup>/PVBTA<sup>n+</sup> and H<sub>2</sub>P<sup>8-</sup>/PVBTA<sup>n+</sup> mixtures leaves the porphyrin fluorescence unchanged during the titration experiments (Figure S4 in the Supporting Information).

On the other hand, when ZnP<sup>8+</sup> and H<sub>2</sub>P<sup>8+</sup> (Scheme 3) were mixed with covalent SWNT-PVBTA<sup>n+</sup>, both components now have the same charge, repulsive interactions resulted in only minor changes in the absorption and/or fluorescence experiments (Figure 6).

These steady-state measurements were further corroborated by time-resolved fluorescence experiments in the absence and presence of variable concentrations of SWNT-



Scheme 3. Positively charged porphyrins utilized as references.

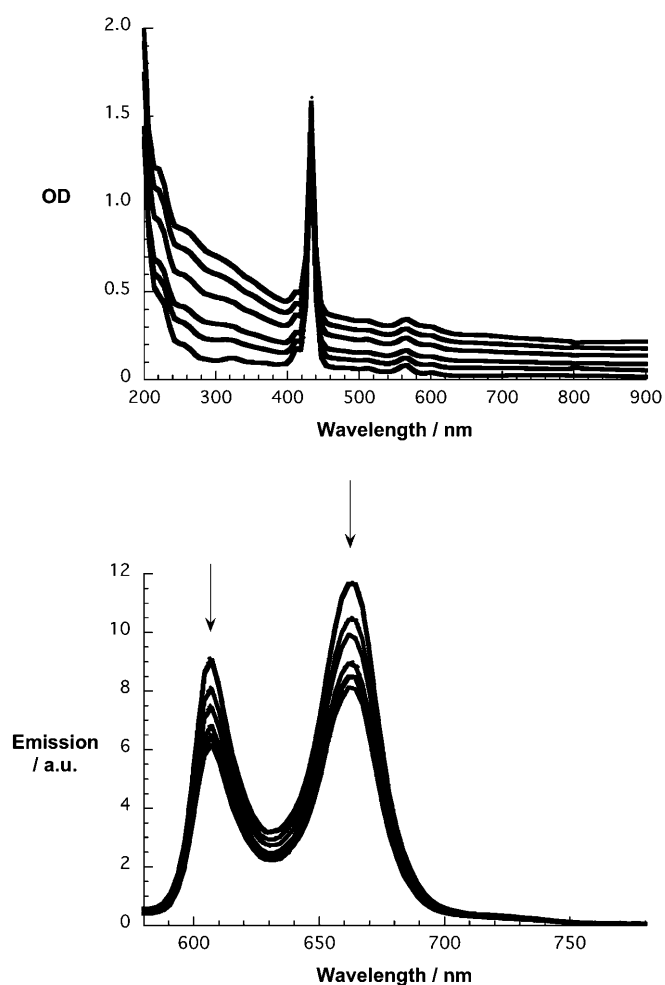


Figure 6. Top: Absorption spectra of a dilute aqueous solution of  $\text{ZnP}^{8+}$  ( $5.0 \times 10^{-6} \text{ M}$ ) with variable concentrations of covalent SWNT-PVBTA $^{n+}$ . Bottom: Steady-state fluorescence spectra of a dilute aqueous solution of  $\text{ZnP}^{8+}$  ( $5.0 \times 10^{-6} \text{ M}$ ) with variable concentrations of SWNT-PVBTA $^{n+}$ . The arrows indicate the progression.

PVBTA $^{n+}$ . The  $\text{ZnP}^{8+}$  fluorescence was followed at 608 nm, whereas that of  $\text{H}_2\text{P}^{8+}$  was monitored at 645 nm. In the absence of SWNT-PVBTA $^{n+}$  the fluorescence decays were best fitted by monoexponential decay functions, giving life-

times of  $(2.4 \pm 0.2)$  and  $(10.1 \pm 0.4)$  ns for  $\text{ZnP}^{8+}$  and  $\text{H}_2\text{P}^{8+}$ , respectively. When SWNT-PVBTA $^{n+}$  was present, the decay traces could no longer be acceptably fitted, giving a  $\chi^2$  value of around one with a simple monoexponential decay function. Instead, the use of biexponential fitting functions was necessary for a satisfactory fit. This yielded a short and long fluorescing lifetime. The long lifetimes are quantitative matches of the intrinsic  $\text{ZnP}^{8+}$

or  $\text{H}_2\text{P}^{8+}$  lifetimes, whereas the short lifetimes (i.e., 0.15 ns) have tentatively been ascribed to intrahybrid deactivations that reflect the expected electron-donor-acceptor interactions.<sup>[27]</sup> Importantly, within tolerable error margins, both lifetimes remain constant, regardless of the composition, that is, the relative ratios between  $\text{ZnP}^{8+}$  and covalent SWNT-PVBTA $^{n+}$  or  $\text{H}_2\text{P}^{8+}$  and covalent SWNT-PVBTA $^{n+}$ .

Protonation of the malonic acid head groups of  $\text{ZnP}^{8+}$  or  $\text{H}_2\text{P}^{8+}$  through the careful addition of acid led to the cancellation of all the effects described above. More precisely, the absorption spectra are now best described as the linear sum of the component spectra; the fluorescence quenching is marginal. In fact, the weak quenching, relative to  $\text{ZnP}^{8+}$  or  $\text{H}_2\text{P}^{8+}$  alone, is primarily caused by competitive light absorption of the different components at the excitation wavelength. Similarly, in time-resolved experiments, only the long-lived components that relate to free and unassociated  $\text{ZnP}^{8+}$  or  $\text{H}_2\text{P}^{8+}$  were found.

In summary, the titration experiments (the absorption and fluorescence assays) indicate the reversible association of  $\text{ZnP}^{8+}$  or  $\text{H}_2\text{P}^{8+}$  with covalent SWNT-PVBTA $^{n+}$ . Electrostatic interactions between oppositely charged head groups favor the formation of novel series of electron-donor-acceptor nanohybrids. In the ground state, weak electronic interactions appear as altered absorption spectra when comparing the component spectra with that of the nanohybrid. Much stronger are the interactions in the excited state in which fast and efficient deactivation of the fluorescing features of both  $\text{ZnP}^{8+}$  and  $\text{H}_2\text{P}^{8+}$  are observed.

To allow a reliable product assignment, we performed 1) ultrafast femtosecond experiments and 2) slower nanosecond experiments. The former were intended to correlate the excited-state deactivation dynamics of  $\text{ZnP}^{8+}$  or  $\text{H}_2\text{P}^{8+}$  with the growth dynamics of any newly formed photoproducts. The objectives of the nanosecond experiments were to determine the long-term stability of the photoproducts.

In the femtosecond experiments (i.e., 150 fs laser pulses at 387 nm) we observed the singlet excited-state features of both porphyrins (data not shown).<sup>[24d]</sup> The singlet features of  $\text{ZnP}^{8+}$  or  $\text{H}_2\text{P}^{8+}$  included transient bleaching of the Soret- and Q-bands in the 400–450 and 500–650 nm regions, respectively.<sup>[25]</sup>

In addition, broad but weak absorptions were seen in the region between 600 and 800 nm. Although the singlet excited states were formed nearly instantaneously (i.e., within  $(1.0 \pm 0.3)$  ps from energetically higher-lying excited states), they were found to be metastable, that is, they slowly decayed on the timescale of our femtosecond experiments. Because the detectable time window is limited to time delays of 1.5 ns, we had to extrapolate the available data to determine the singlet lifetimes (i.e.,  $\text{ZnP}^{8-}$ :  $(2.2 \pm 0.2)$  ns;  $\text{H}_2\text{P}^{8-}$ :  $(9.8 \pm 1.0)$  ns). The products of these singlet decays are the corresponding triplet states that are generated through an efficient intersystem crossing in both cases (see below).

Initially upon photoexciting  $\text{ZnP}^{8-}/\text{SWNT-PVBTA}^{n+}$  or  $\text{H}_2\text{P}^{8-}/\text{SWNT-PVBTA}^{n+}$  we saw the same singlet attributes that we observed for  $\text{ZnP}^{8-}$  or  $\text{H}_2\text{P}^{8-}$ , respectively (see Figure 7). Such observations are fundamental because they attest to the photoexcitation of the two chromophores.<sup>[28]</sup>

The presence of covalent  $\text{SWNT-PVBTA}^{n+}$ , however, has a significant impact on the singlet excited decays of  $\text{ZnP}^{8-}$  or  $\text{H}_2\text{P}^{8-}$ . Much shorter lifetimes, which are now of the order of 0.05 ns, point to expedited singlet decays. Moreover, these lifetimes agree well with the values derived from

the time-resolved fluorescence measurements. No particular resemblance was found when comparing the transients recorded at the conclusion of the accelerated singlet decays of  $\text{ZnP}^{8-}/\text{SWNT-PVBTA}^{n+}$  or  $\text{H}_2\text{P}^{8-}/\text{SWNT-PVBTA}^{n+}$  with those of  $\text{ZnP}^{8-}$  or  $\text{H}_2\text{P}^{8-}$  alone. This dissimilarity holds equally for the corresponding singlet and triplet excited-state features. The most dominant characteristics of the new products are maxima at 460 and 700 nm in the visible range. These distinctly broad absorptions are quite characteristic of an electron-transfer product involving either  $\text{ZnP}^{8-}$  or  $\text{H}_2\text{P}^{8-}$ .<sup>[24d]</sup> Also important is the range beyond 1000 nm (i.e., 1000–1600 nm), which immediately after photoexcitation is dominated by a negative imprint of the van Hove singularities. These spectral characteristics transform into a new product. In particular, an appreciable blueshift of the transient with a minimum at 1020 nm was detected. Implicit are new conduction band electrons, injected from photoexcited  $\text{ZnP}^{8-}$  or  $\text{H}_2\text{P}^{8-}$ , which shifts the transitions to lower energies. In line with previous reports we postulate charge-transfer interactions between photoexcited  $\text{ZnP}^{8-}$  or  $\text{H}_2\text{P}^{8-}$  and SWNTs.<sup>[25]</sup>

In accordance with the femtosecond experiments, nanosecond excitation (i.e., 5 ns laser pulses at 532 or 355 nm) of solutions of  $\text{ZnP}^{8-}$  or  $\text{H}_2\text{P}^{8-}$  in the absence of SWNTs revealed exclusively triplet characteristics that evolve, as shown above, as a result of rapid intersystem crossing processes.<sup>[24d]</sup> These spectra are characterized by transient maxima in the 750–850 nm range.

In particular, 840 nm is the maximum for  $\text{ZnP}^{8-}$ , whereas for  $\text{H}_2\text{P}^{8-}$  the maximum is slightly blueshifted and is found at 780 nm. In the absence of molecular oxygen the triplet lifetimes are substantial with values of around 50  $\mu\text{s}$ . On the other hand, admitting variable concentrations of molecular oxygen to these solutions resulted in the diffusion-controlled formation of singlet oxygen.<sup>[29]</sup>

Quite different were the changes that we recorded for  $\text{ZnP}^{8-}/\text{SWNT-PVBTA}^{n+}$  or  $\text{H}_2\text{P}^{8-}/\text{SWNT-PVBTA}^{n+}$ . Instead of registering the triplet features of  $\text{ZnP}^{8-}$  or  $\text{H}_2\text{P}^{8-}$ , we observed broad transitions that resembled those of the one-electron oxidized  $\pi$ -radical cations of either porphyrin. These radical ion features, as displayed in Figure 8, evolve from intrahybrid electron-transfer quenching. From an analysis of the decays at various wavelengths the radical ion-pair lifetimes were determined as 2.2  $\mu\text{s}$ .

For the construction of nanostructured photoelectrodes we took advantage of our previous experience with the electrostatically driven layer-by-layer (LBL) deposition technique.<sup>[24c,e,30]</sup> Quartz slides, indium tin oxide (ITO) electrodes, and mica wafers were used as substrates to conduct optical characterization, photocurrent measurements, and AFM imaging, respectively. Prior to their use, all substrates were treated with poly(diallyldimethylammonium chloride) (PDDA) to make them more hydrophilic. Once the surface is sufficiently overlaid with PDDA, the substrates can interact with  $\text{SWNT-PVBTA}^{n+}$  or  $\text{SWNT/PVBTA}^{n+}$ . In the final step,  $\text{ZnP}^{8-}$  (i.e., aqueous solution, pH 11.2) was electrostatically deposited onto the  $\text{PVBTA}^+$ . At the end of this se-

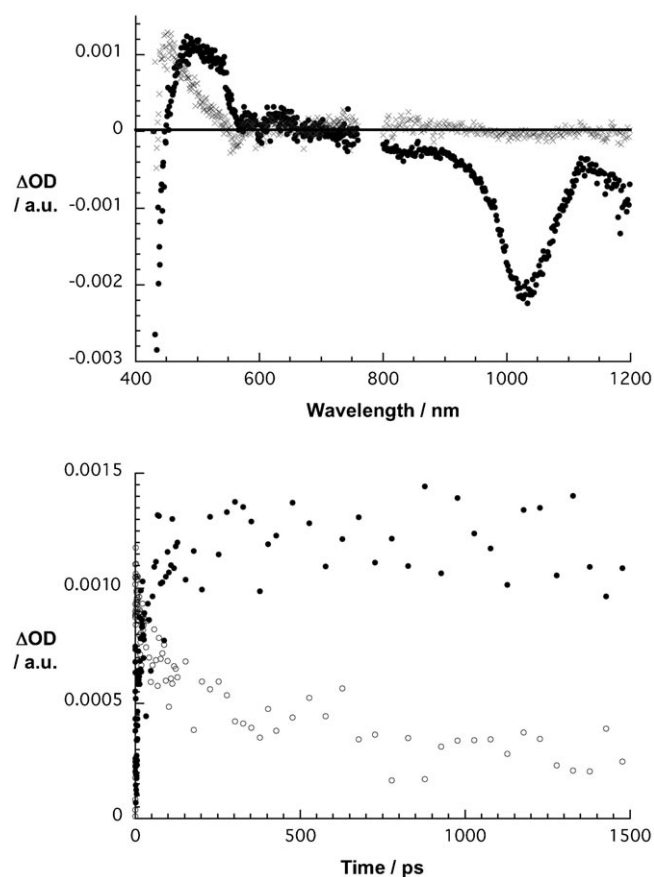


Figure 7. Top: Differential absorption spectra (visible and near-infrared) obtained upon femtosecond flash photolysis (387 nm) of covalent  $\text{SWNT-PVBTA}^{n+}$  and  $\text{ZnP}^{8-}$  ( $5.0 \times 10^{-6}$  M) in  $\text{D}_2\text{O}$  at room temperature with time delays of 1.8 (●) and 1000 ps (×). Bottom: Time-absorption profiles of the spectra shown in the upper part at 450 (●) and 525 nm (○) monitoring the formation of the radical ion pair.

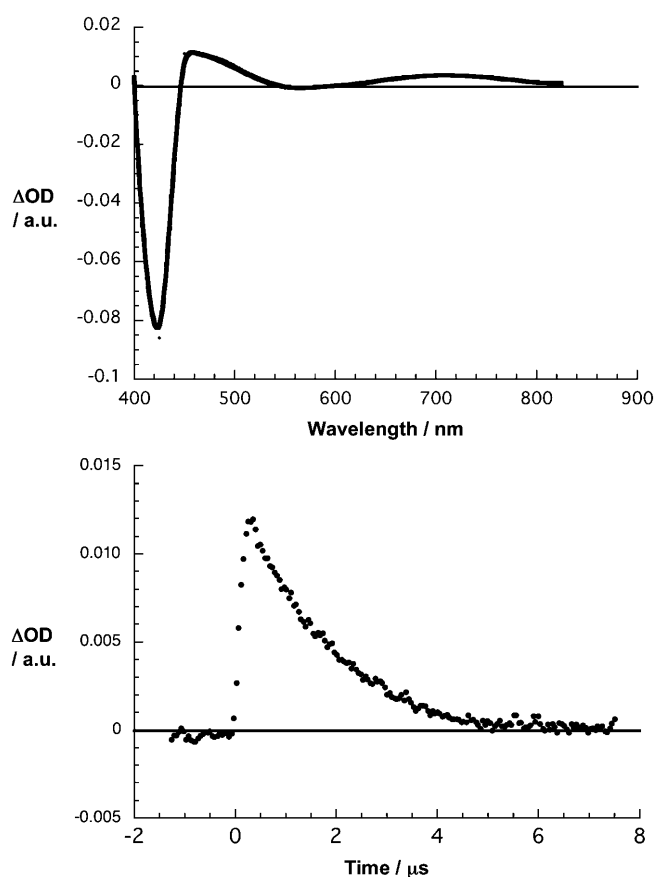


Figure 8. Top: Differential absorption spectrum (visible) obtained upon nanosecond flash photolysis (532 nm) of SWNT-PVBTA<sup>n+</sup> and ZnP<sup>8-</sup> ( $5.0 \times 10^{-6}$  M) in D<sub>2</sub>O with a time delay of 100 ns. Bottom: Time-absorption profiles of the spectrum shown in the upper part at 455 nm monitoring the decay of the radical ion pair.

quential deposition, PDDA/SWNT-PVBTA<sup>n+</sup>/ZnP<sup>8-</sup> and PDDA/SWNT/PVBTA<sup>n+</sup>/ZnP<sup>8-</sup> nanocomposites had been constructed on the solid substrates (i.e., quartz, ITO, and mica wafers).

Evidence for the successful deposition came from absorption spectra, which were recorded after the completion of each deposition step (an example is shown in Figure S5 in the Supporting Information). As in previous LBL SWNT cases, which were independently characterized by ellipsometry of the film thickness, the absorption spectra showed that each deposition step is basically limited to a monolayer coverage.<sup>[30a,31]</sup>

Immediately after their preparation, the modified ITO electrodes were photoelectrochemically characterized by applying the following conditions: 0.1 M Na<sub>3</sub>PO<sub>4</sub> and 5 mM ascorbic acid after nitrogen bubbling. Typical current-voltage characteristics using an Ag/AgCl (0.1 M KCl) reference electrode are reported in Figure 9 and photoaction spectra without an applied potential are reported in Figure 10.

From the latter we deduce IPCE values of 3.32 and 5.80% for PDDA/SWNT-PVBTA<sup>n+</sup>/ZnP<sup>8-</sup> and PDDA/SWNT/PVBTA<sup>n+</sup>/ZnP<sup>8-</sup>, respectively. For comparison, the maximum IPCE values obtained for our previously tested

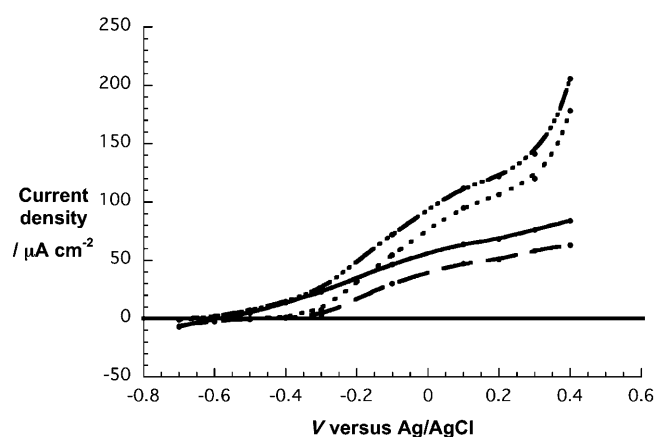


Figure 9. Current-voltage characteristics of the ITO/PDDA/SWNT-PVBTA<sup>n+</sup>/ZnP<sup>8-</sup> (solid spectrum: photocurrent; dashed spectrum: dark current) and ITO/PDDA/SWNT/PVBTA<sup>n+</sup>/ZnP<sup>8-</sup> (solid/dotted spectrum: photocurrent; dotted spectrum: dark current) photoelectrodes.

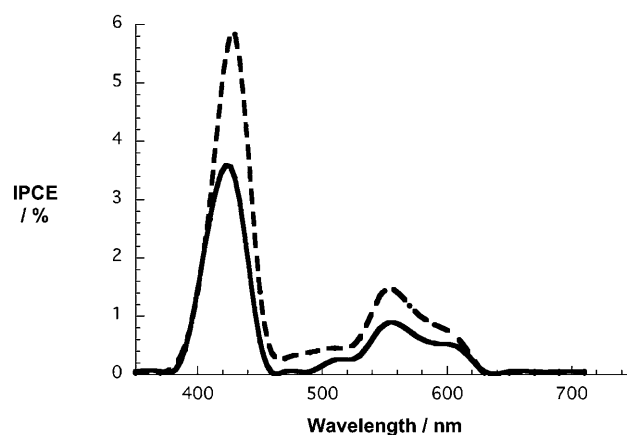


Figure 10. Photoaction spectra of the ITO/PDDA/SWNT-PVBTA<sup>n+</sup>/ZnP<sup>8-</sup> (solid spectrum) and ITO/PDDA/SWNT/PVBTA<sup>n+</sup>/ZnP<sup>8-</sup> (dashed spectrum) photoelectrodes.

ITO/PDDA/SWNT/pyrene<sup>+</sup>/ZnP<sup>8-</sup> and ITO/PDDA/SWNT-PSS<sup>-</sup>/ZnP<sup>8+</sup> photoelectrodes were 1.8 and 0.25%, respectively.<sup>[22]</sup> Further characteristics of PDDA/SWNT-PVBTA<sup>n+</sup>/ZnP<sup>8-</sup> are  $V_{OC} = -0.57$  V and  $i_{SC} = 16.7 \mu A cm^{-2}$ , whereas for PDDA/SWNT/PVBTA<sup>n+</sup>/ZnP<sup>8-</sup>  $V_{OC} = -0.59$  V and  $i_{SC} = 17.3 \mu A cm^{-2}$ . When facilitating the charge collection at the ITO electrode, that is, applying a bias of +0.5 V, the IPCE values show a remarkable improvement to 3.81 and 9.90% for PDDA/SWNT-PVBTA<sup>n+</sup>/ZnP<sup>8-</sup> and PDDA/SWNT/PVBTA<sup>n+</sup>/ZnP<sup>8-</sup>, respectively.

We believe that the PDDA/SWNT/PVBTA<sup>n+</sup>/ZnP<sup>8-</sup> cell is more effective, in terms of photocurrent efficiency, due to the presence of a charge gradient. Shorter distances between ZnP<sup>8-</sup> and SWNTs as well as between SWNTs and ITO might also be responsible for the better performance. Here, enhanced hydrophobic interactions between the modified, hydrophobic ITO surface, the PDDA polymer layer, and the positively charged SWNTs are of particular importance.<sup>[32]</sup> It is notable that, for the present study, CoMoCat SWNTs

were employed, whereas our previous work was based solely on HiPco SWNTs. However, a comparison of the highest efficient PDDA/SWNT/PVBTA<sup>n+</sup>/ZnP<sup>s-</sup> cells with CoMoCat and HiPco SWNTs produced no notable differences.

## Conclusion

The present work underlines the benefits of employing covalent SWNT–PVBTA<sup>n+</sup> and/or noncovalent SWNT/PVBTA<sup>n+</sup> as integrative components for novel organic photoelectrochemical solar cells that show improved photoconversion efficiency. The approach is simple and relies on electrostatic interactions: polyanionic porphyrins (photoexcited-state electron donors) interact with the positively charged trimethylammonium head groups of the polymer chains grafted onto the surface of SWNTs or wrapped around them (as ground-state electron acceptors) to afford SWNT/PVBTA<sup>n+</sup>/ZnP<sup>s-</sup> nanocomposites.

Utilization of polymer-grafted or -wrapped SWNTs guarantees considerable dispersibility even in aqueous solutions without, however, compromising the electronic structure of the SWNTs. Although this aspect appears to be general, the presence of a charge gradient is unique to PVBTA<sup>n+</sup>. This charge gradient has emerged as a powerful means to facilitate charge injection from photoexcited porphyrins to SWNTs. The benefits are as follows: photoexcitation in solution/D<sub>2</sub>O resulted in the rapid (i.e., 0.15 ns) generation of radical ion pairs with one of the longest lifetimes (i.e., 2.2 μs) ever recorded for such nanohybrid systems and at photoelectrodes/ITO the highest monochromatic photoconversion efficiency (i.e., 9.90% at a bias of +0.5 V) seen so far for a single sandwich-layered device.

## Experimental Section

**General:** Femtosecond transient absorption studies were performed with 387 nm laser pulses (1 kHz, 150 fs pulse width) from an amplified Ti:sapphire laser system (Clark-MXR). Nanosecond laser flash photolysis experiments were performed with 532 nm laser pulses from a nitrogen laser (8 ns pulse width) in a front-face excitation geometry. Fluorescence lifetimes were measured with a laser Strobe fluorescence lifetime spectrometer (Photon Technology International) with 337 nm laser pulses from a nitrogen laser fiber coupled to a lens-based T-formal sample compartment equipped with a stroboscopic detector. Details of the Laser Strobe systems are described on the manufacturer's web site. Emission spectra were recorded by using a FluoroMax-3 spectrophotometer (Horiba Company). The experiments were performed at room temperature. Each spectrum represents an average of at least five individual scans and appropriate corrections were applied whenever necessary. Photoelectrochemical measurements were carried out in a three-arm cell with working (ITO), counter (platinum gauze), and reference (Ag/AgCl) electrodes (only when a bias voltage, from a Princeton Applied Research, model 175 galvanostat/potentiostat, was applied). The sacrificial electron donor was 5 mM sodium ascorbate in 0.1 M Na<sub>3</sub>PO<sub>4</sub> (pH 12) and N<sub>2</sub> was bubbled into the solution for 10–15 min prior to the photoelectrochemical measurements. Photocurrent measurements were carried out by using a Keithley model 2400 programmable multimeter immediately after illumination. A collimated light beam from a xenon lamp provided with an AM1.5

filter was used for the solar radiation illumination. When white light was used, a 375 nm cut filter was used. To record the photoaction spectra, a Bausch and Lomb high-intensity grating monochromator was introduced into the path of the excitation beam to select the required wavelengths. All measurements were taken after subtracting the stable dark current. The IPCE, defined as the number of electrons collected per incident photon, was evaluated from short circuit photocurrent measurements at different wavelengths versus the photocurrent measured by using a photodiode of the type PIN UV 100 (UDT Sensors).

**TEM analysis:** A drop of a solution of covalent SWNT–PVBTA<sup>n+</sup> was placed on a copper grid (3.00 mm, 200 mesh). After vacuum drying overnight (10<sup>-2</sup> bar), the sample was observed with a TEM Philips EM 208 microscope (accelerating voltage of 100 kV).

**AFM analysis:** The samples were prepared by spin-coating onto silicon wafers from a solution of covalent SWNT–PVBTA<sup>n+</sup> in water and then investigated by using Digital Instruments (Veeco) Nanoscope IIIa (Tapping Mode) with Veeco RTESP7 Tips.

**Polymerization of VBTA with SWNTs:** A mixture of VBTA monomer (4.0 g), carbon nanotubes (40 mg; CoMoCat from Southwest Nanotechnologies, Norman, OK, USA), and deionized water (65 mL of) in a 100 mL Schlenk flask was sonicated for 15 min and then stirred for 4 h. Then VA-044 initiator (2,2'-azobis[2-(2-imidazolin-2-yl)propane] dihydrochloride; 48 mg) was added. The mixture was degassed under vacuum and refilled with nitrogen three times. The mixture was degassed once more and heated with stirring in an oil bath at 75 °C for 48 h. The mixture was cooled to 25 °C, opened to the air, diluted to 500 mL with water, sonicated for 1 h, and centrifuged at 5000g for 6 h. The resulting black supernatant liquid was removed. The black sediment was redispersed in water by stirring and the centrifugation procedure was repeated two more times. The combined supernatants were concentrated by ultrafiltration through a 0.45 μm cellulose acetate membrane under 10 psi pressure until the volume was reduced to 60 mL. The concentrated suspension was centrifuged at 200000g for 2 h to precipitate the SWNTs. The solution containing residual free polymer was decanted. The precipitate was redispersed in water and the centrifugation procedure was repeated two more times at 200000g. The resulting black precipitate was redispersed in water (100 mL). The concentration of SWNT–polymer in this dispersion was estimated gravimetrically to be 53 mg L<sup>-1</sup> SWNTs. Based on the C/N ratio determined by elemental analysis the SWNT/PVBTA ratio was estimated to be 62:38 by weight. For the optical spectroscopic studies, 50 mL of the 53 mg L<sup>-1</sup> dispersion was centrifuged at 40000g for 100 min and 20 mL of the supernatant was removed for analysis. Based on its optical density, the concentration of SWNTs in the supernatant was 5.3 mg L<sup>-1</sup>.

**Preparation of the SWNT/PVBTA<sup>n+</sup> mixture suspension:** SWNTs (1 mg) and PVBTA<sup>n+</sup> (6 mg) were suspended in Millipore water (6 mL), stirred overnight, sonicated for 6 h, centrifuged for 30 min at 10000 rpm, and then the supernatant was taken.

## Acknowledgements

This work was carried out with partial support from the European Union (RTN networks "WONDERFULL" and "CASSIUSCLAYS"), the University of Trieste and MUR (PRIN 2006, prot. 2006034372, and Fibr RBIN04HC3S), the Deutsche Forschungsgemeinschaft (SFB 583, Gu517/4-1, and Ju323/5-1), the Fonds der Chemischen Industries, National Science Foundation grant EPS-0132543 and EPS-0447262 (WTF), and the Office of Basic Energy Sciences of the U.S. Department of Energy. Mr. Claudio Gamboz (Centro Servizi Polivalenti di Ateneo, Università di Trieste) is gratefully acknowledged for assistance with TEM imaging.

- [1] a) S. J. M. Tans, M. H. Devoret, H. Dai, A. Thess, R. E. Smalley, L. J. Geerligs, C. Dekker, *Nature* **1997**, *386*, 474; b) J. Kong, N. R. Franklin, C. W. Zhou, M. G. Chapline, S. Peng, K. J. Cho, H. Dai, *Science* **2000**, *287*, 622; c) A. Goldoni, R. Lariciprete, L. Petaccia, S.



- Lizzit, *J. Am. Chem. Soc.* **2003**, *125*, 11329; d) D. Dietzel, M. Faucher, A. Iaia, J. P. Aime, S. Marsaudon, A. M. Bonnot, V. Bouchiat, G. Couturier, *Nanotechnology* **2005**, *16*, S73; e) T. Fukushima, A. Kosaka, Y. Yamamoto, T. Aimiya, S. Notazawa, T. Takigawa, T. Inabe, T. Aida, *Small* **2006**, *2*, 554; f) R. Haggemueller, H. H. Gommans, A. G. Rinzler, J. E. Fischer, K. I. Winey, *Chem. Phys. Lett.* **2000**, *330*, 219; g) A. Mierczynska, M. Mayne-L'Hermite, G. Boiteux, J. K. Jeszka, *J. Appl. Polym. Sci.* **2007**, *105*, 158; h) T.-E. Chang, A. Kisliuk, S. M. Rhodes, W. J. Brittain, A. P. Sokolov, *Polymer* **2006**, *47*, 7740.
- [2] a) R. H. Baughman, C. X. Cui, A. A. Zahidov, Z. Iqbal, J. N. Barisci, G. M. Spinks, G. G. Wallace, A. Mazzoldi, D. De Rossi, A. G. Rinzler, O. Jaszinski, S. Roth, M. Kertesz, *Science* **1999**, *284*, 1340; b) A. A. Mamedov, N. A. Kotov, M. Prato, D. M. Guldi, J. P. Wicksted, A. Hirsch, *Nat. Mater.* **2002**, *1*, 190; c) A. B. Dalton, S. Collins, E. Munoz, J. M. Razal, V. H. Ebron, J. P. Ferraris, J. N. Coleman, B. G. Kim, R. H. Baughman, *Nature* **2003**, *423*, 703; d) L. C. Teague, S. Banerjee, S. S. Wong, C. A. Richter, B. Varughese, J. D. Batteas, *Chem. Phys. Lett.* **2007**, *442*, 354; e) Y. F. Li, R. Hatakeyama, T. Kaneko, T. Izumida, T. Okada, T. Kato, *Appl. Phys. Lett.* **2006**, *89*, 083117/1; f) U. Dettlaff-Weglikowska, V. Skakalova, R. Graupner, S. H. Jhang, B. H. Kim, H. J. Lee, L. Ley, Y. W. Park, S. Berber, D. Tomanek, S. Roth, *J. Am. Chem. Soc.* **2005**, *127*, 5125; g) J. Cao, Q. Wang, H. Dai, *Phys. Rev. Lett.* **2003**, *90*, 157601; h) S. Li, Z. Yu, C. Rutherglen, P. J. Burke, *Nano Lett.* **2004**, *4*, 2003; i) E. Kymakis, G. A. J. Amaratunga, *J. Appl. Phys.* **2006**, *99*, 084302/1.
- [3] a) D. C. Sorescu, K. D. Jordan, P. Avouris, *J. Phys. Chem. B* **2001**, *105*, 11227; b) A. Javey, J. Guo, Q. Wang, M. Lundstrom, H. Dai, *Nature* **2003**, *424*, 654; c) Y. Zhang, H. Son, J. Zhang, J. Kong, Z. Liu, *J. Phys. Chem. C* **2007**, *111*, 1988; d) S. B. Cronin, Y. Yin, A. Walsh, R. B. Capaz, A. Stolyarov, P. Tangney, M. L. Cohen, S. G. Louie, A. K. Swan, M. S. Unlu, B. B. Goldberg, M. Tinkham, *Phys. Rev. Lett.* **2006**, *96*, 127403/1; e) M. S. Dresselhaus, G. Dresselhaus, A. Jorio, *Ann. Rev. Mater. Res.* **2004**, *34*, 247; f) L. Vivien, P. Lancon, D. Riehl, F. Hache, E. Anglaret, *Carbon* **2002**, *40*, 1789.
- [4] a) P. Avouris, *Acc. Chem. Res.* **2002**, *35*, 1026; b) P. G. Collins, P. Avouris, *Sci. Am.* **2000**, *283*, 62; c) T. Yildirim, O. Gulseren, S. Ciraci, *Phys. Rev. B* **2001**, *64*, 075404/1; d) J. Jiang, K. Liu, W. Lu, Y. Luo, *J. Chem. Phys.* **2006**, *124*, 214711/1; e) H. M. Moghaddam, S. A. Ketabi, N. Shahtahmasebi, *J. Appl. Phys.* **2007**, *19*, 116211/1.
- [5] a) P. Qi, A. Javey, M. Rolandi, Q. Wang, E. Yenilmez, H. Dai, *J. Am. Chem. Soc.* **2004**, *126*, 11774; b) G. W. Peng, A. C. H. Huan, Y. P. Feng, *Appl. Phys. Lett.* **2006**, *88*, 193117/1; c) P. J. de Pablo, C. Gomez-Navarro, A. Gil, J. Colchero, M. T. Martinez, A. M. Benito, W. K. Maser, J. Gomez-Herrero, A. M. Baro, *Appl. Phys. Lett.* **2001**, *79*, 2979; d) N. R. Wilson, J. V. MacPherson, *Nano Lett.* **2003**, *3*, 1365; e) S. Lu, K. Sivakumar, B. Panchapakesan, *J. Nanosci. Nanotechnol.* **2007**, *7*, 2473.
- [6] a) T. Takenobu, Y. Murayama, Y. Iwasa, *Appl. Phys. Lett.* **2006**, *89*, 263510/1; b) H. R. Byon, H. C. Choi, *J. Am. Chem. Soc.* **2006**, *128*, 2188; c) S. J. Tans, A. R. M. Verschneesen, C. Dekker, *Nature* **1998**, *393*, 49.
- [7] a) P. Qi, O. Vermesh, M. Gurecu, A. Javey, Q. Wang, H. Dai, S. Peng, K. J. Cho, *Nano Lett.* **2003**, *3*, 347; b) A. Star, T. R. Han, J. C. Gabriel, K. Bradley, P. Gruner, *Nano Lett.* **2003**, *3*, 459; c) S. Liu, C. Cai, *J. Electroanal. Chem.* **2007**, *602*, 103; d) Y. Wang, P. P. Joshi, K. L. Hobbs, M. B. Johnson, D. W. Schmidtke, *Langmuir* **2006**, *22*, 9776.
- [8] a) T. Rueckes, K. Kim, E. Joselevich, G. Y. Tseng, C. L. Cheunh, C. M. Lieber, *Science* **2000**, *289*, 94; b) J. W. Kang, H. J. Hwang, *Comput. Mater. Sci.* **2005**, *33*, 338.
- [9] a) H. Dai, *Surf. Sci.* **2002**, *500*, 218; b) L. M. Dai, A. Patil, X. Y. Gong, Z. X. Guo, L. Q. Lin, Y. Liu, D. B. Zhu, *ChemPhysChem* **2003**, *4*, 1150; c) R. Song, Z. Jiang, W. Bi, W. Cheng, J. Lu, B. Huang, T. Tang, *Chem. Eur. J.* **2007**, *13*, 3234.
- [10] a) B. Q. Wei, R. Vajtai, Y. Jung, J. Ward, R. Zhang, G. Ramanath, P. M. Ajayan, *Nature* **2002**, *416*, 495; b) V. Z. Mordkovich, E. A. Dolgova, A. R. Karaeva, D. N. Kharitonov, I. A. Maslov, A. A. Kamenev, V. F. Tretjakov, *Carbon* **2007**, *45*, 62.
- [11] a) D. Tasis, N. Tagmatarchis, V. Georgakilas, M. Prato, *Chem. Eur. J.* **2003**, *9*, 4001; b) O. Matarredona, H. Rhoads, Z. Li, J. H. Harwell, L. Balzano, D. E. Resasco, *J. Phys. Chem. B* **2003**, *107*, 13357; c) Z. Yao, N. Braid, G. A. Botton, A. Adronov, *J. Am. Chem. Soc.* **2003**, *125*, 16015; d) T. G. Hedderman, S. M. Keogh, G. Chambers, H. J. Byrne, *J. Phys. Chem. B* **2004**, *108*, 18860.
- [12] a) S. Niyogi, M. A. Hamon, H. Hu, B. Zhao, P. Bhowmik, R. Sen, M. E. Itkis, R. C. Haddon, *Acc. Chem. Res.* **2002**, *35*, 1105; b) S. Banerjee, T. Hemraj-Benny, S. Wang, *Adv. Mater.* **2005**, *17*, 17; c) D. Tasis, N. Tagmatarchis, A. Bianco, M. Prato, *Chem. Rev.* **2006**, *106*, 1105; d) J. J. Davis, K. S. Coleman, B. R. Azamian, C. B. Bagshaw, M. L. H. Green, *Chem. Eur. J.* **2003**, *9*, 3732; e) B. L. Fletcher, T. E. McKnight, A. V. Melechko, M. L. Simpson, M. Doktycz, *J. Nanotech.* **2006**, *17*, 2032; f) M. Holzinger, O. Vostrowsky, A. Hirsch, F. Hennrich, M. Kappes, R. Weiss, F. Jellen, *Angew. Chem.* **2001**, *113*, 4132; *Angew. Chem. Int. Ed.* **2001**, *40*, 4002; g) J. Li, H. Grennberg, *Chem. Eur. J.* **2006**, *12*, 3869.
- [13] a) N. Nakashima, Y. Tomonari, H. Murakami, *Chem. Lett.* **2002**, 638; b) D. M. Guldi, G. M. A. Rahman, N. Jux, N. Tagmatarchis, M. Prato, *Angew. Chem.* **2004**, *116*, 5642; *Angew. Chem. Int. Ed.* **2004**, *43*, 5526; c) R. J. Chen, Y. Zhang, D. Wang, H. Dai, *J. Am. Chem. Soc.* **2001**, *123*, 3838; d) R. J. Chen, S. Bangsaruntip, K. A. Drouvalakis, N. W. S. Kam, M. Shim, Y. M. Li, W. Kim, P. J. Utz, H. Hai, *Proc. Natl. Acad. Sci. USA* **2003**, *100*, 4984; e) L. Liu, T. Wang, J. Li, Z. Guo, L. M. Dai, D. Zhang, D. Zhu, *Chem. Phys. Lett.* **2003**, *367*, 747; f) F. J. Gomez, R. J. Chen, D. Wang, R. M. Waymouth, H. Dai, *Chem. Commun.* **2003**, 190; g) J. J. Davis, K. S. Coleman, B. R. Azamian, C. B. Bagshaw, M. L. H. Green, *Chem. Eur. J.* **2003**, *9*, 3732; h) B. L. Fletcher, T. E. McKnight, A. V. Melechko, M. L. Simpson, M. J. Doktycz, *Nanotechnology* **2006**, *17*, 2032; i) M. Holzinger, O. Vostrowsky, A. Hirsch, F. Hennrich, M. Kappes, R. Weiss, F. Jellen, *Angew. Chem.* **2001**, *113*, 4132; *Angew. Chem. Int. Ed.* **2001**, *40*, 4002; j) J. Li, H. Grennberg, *Chem. Eur. J.* **2006**, *12*, 3869.
- [14] a) A. B. Dalton, C. Stephan, J. N. Coleman, B. McCarthy, P. M. Ajayan, S. Lefrant, P. Bernier, W. J. Blau, H. J. Byrne, *J. Phys. Chem. B* **2000**, *104*, 10012; b) A. Star, J. F. Stoddart, D. Steurman, M. Diehl, A. Boukai, E. W. Wong, X. Yang, S. W. Chung, H. Choi, J. R. Heath, *Angew. Chem.* **2001**, *113*, 1771; *Angew. Chem. Int. Ed.* **2001**, *40*, 1721; c) M. J. O'Connell, P. Boul, L. M. Ericson, C. Huffman, Y. Wang, E. Haroz, C. Kuper, J. M. Tour, K. D. Ausman, R. E. Smalley, *Chem. Phys. Lett.* **2001**, *342*, 265; d) J. Chen, H. Liu, W. A. Weimer, M. D. Halls, D. H. Waldeck, G. C. Walker, *J. Am. Chem. Soc.* **2002**, *124*, 9034.
- [15] a) Y. P. Sun, K. F. Fu, Y. Lin, W. Huang, J. *Acc. Chem. Res.* **2002**, *35*, 1096; b) D. E. Hill, Y. Lin, A. M. Rao, L. F. Allard, Y. P. Sun, *Macromolecules* **2002**, *35*, 9466; c) I. Cotiuga, F. Picchioni, U. S. Agarwal, B. B. P. Staal, A. J. M. Vekemans, P. J. Lemstra, *Macromol. Rapid Commun.* **2006**, *27*, 242; d) J. Zhu, H. Peng, F. Rodriguez-Macias, J. L. Margrave, V. N. Khabashesku, A. M. Imam, K. Lozano, E. V. Barrera, *Adv. Funct. Mater.* **2004**, *14*, 643.
- [16] a) F. Pompeo, D. E. Resasco, *Nano Lett.* **2002**, *2*, 369; b) M. G. C. Kahn, S. Banerjee, S. S. Wong, *Nano Lett.* **2002**, *2*, 1215; c) X. J. Huang, H. S. Im, D. H. Lee, H. S. Kim, Y. K. Choi, *J. Phys. Chem. C* **2007**, *111*, 1200.
- [17] a) V. Georgakilas, N. Tagmatarchis, D. Pantarotto, A. Bianco, J. P. Briand, M. Prato, *Chem. Commun.* **2002**, 3050; b) T. Ramanathan, F. T. Fisher, R. S. Rouff, L. C. Brinson, *Chem. Mater.* **2005**, *17*, 1290; c) C. A. Dyke, M. P. Stewart, F. Maya, J. M. Tour, *Synlett* **2004**, *1*, 155; d) H. T. Ham, Y. S. Choi, I. J. Chung, *J. Colloid Interface Sci.* **2005**, *286*, 216.
- [18] a) J. Q. Liu, T. Xiao, K. Liao, P. Wu, *Nanotechnology* **2007**, *18*, 165701/1; b) J. Chen, R. Ramasubramaniam, C. Xue, H. Liu, *Adv. Funct. Mater.* **2006**, *16*, 114; c) Z. Li, Y. Dong, M. Haussler, J. W. Y. Lam, Y. Dong, L. Wu, K. S. Wong, B. Z. Tang, *J. Phys. Chem. B* **2006**, *110*, 2302; d) H. Li, F. Cheng, A. M. Duft, A. Adronov, *J. Am. Chem. Soc.* **2005**, *127*, 14524; e) J. L. Bahr, J. M. Tour, *J. Mater. Chem.* **2002**, *12*, 1952; f) T. Ramanathan, F. T. Fisher, R. S. Ruoff, L. C. Brinson, *Chem. Mater.* **2005**, *17*, 1290.

- [19] a) A. Hirsch, *Angew. Chem.* **2002**, *114*, 1933; *Angew. Chem. Int. Ed.* **2002**, *41*, 1853; b) J. L. Bahr, J. M. Tour, *J. Mater. Chem.* **2002**, *12*, 1952; c) S. Banerjee, M. G. C. Kahn, S. S. Wang, *Chem. Eur. J.* **2003**, *9*, 1898; d) D. Tasis, N. Tagmatarchis, V. Georgakilas, M. Prato, *Chem. Eur. J.* **2003**, *9*, 4000; e) C. A. Dyke, J. M. Tour, *Chem. Eur. J.* **2004**, *10*, 813; f) S. Banerjee, T. Hemraj-Benny, S. S. Wong, *Adv. Mater.* **2005**, *17*, 17; g) N. Tagmatarchis, M. Prato, *J. Mater. Chem.* **2004**, *14*, 437; h) A. Bianco, M. Prato, *Adv. Mater.* **2003**, *15*, 1765.
- [20] a) H. Geng, R. Rosen, B. Zheng, H. Shimoda, L. Fleming, J. Liu, O. Zhou, *Adv. Mater.* **2002**, *14*, 1387; b) C. A. Mitchell, J. L. Bhar, S. Arepalli, J. M. Tour, R. Krishnamoorti, *Macromolecules* **2002**, *35*, 8825; c) G. Viswanathan, N. Chakrapani, H. Yang, B. Wei, H. Chung, K. Cho, C. Y. Ryu, P. M. Ajayan, *J. Am. Chem. Soc.* **2003**, *125*, 9258; d) Y. Lin, B. Zhou, K. A. Fernando, P. Shiral Liu, L. F. Allard, Y. P. Sun, *Macromolecules* **2002**, *35*, 8825; e) J. Zhu, H. Peng, F. Rodriguez-Macias, J. L. Margrave, V. N. Khabashesku, A. M. Imam, K. Lozano, E. V. Barrera, *Adv. Funct. Mater.* **2004**, *14*, 643; f) L. Liu, A. H. Barber, S. Nuriel, H. D. Wagner, *Adv. Funct. Mater.* **2005**, *15*, 643; g) S. Qin, D. Qin, W. T. Ford, D. E. Resasco, J. E. Herrera, *J. Am. Chem. Soc.* **2004**, *126*, 170; h) F. Cheng, A. Adronov, *Chem. Eur. J.* **2006**, *12*, 5053; i) K. I. Winey, T. Kashiwagi, M. Mu, *MRS Bull.* **2007**, *32*, 348; j) P. M. Ajayan, J. M. Tour, *Nature* **2007**, *447*, 1066.
- [21] a) H. Imahori, Y. Sakata, *Adv. Mater.* **1997**, *9*, 537; b) M. Prato, *J. Mater. Chem.* **1997**, *7*, 1097; c) N. Martin, L. Sanchez, B. Illescas, I. Perez, *Chem. Rev.* **1998**, *98*, 2527; d) F. Diederrich, M. Gomez-Lopez, *Chem. Soc. Rev.* **1999**, *28*, 263; e) D. M. Guldi, *Chem. Commun.* **2000**, 321; f) D. M. Guldi, M. Prato, *Acc. Chem. Res.* **2000**, *33*, 695; g) D. Gust, T. A. Moore, A. L. Moore, *Acc. Chem. Res.* **2001**, *34*, 40; h) D. M. Guldi, *Chem. Soc. Rev.* **2002**, *31*, 22; i) D. M. Guldi, M. Prato, *Chem. Commun.* **2004**, 2571; j) J. L. Segura, N. Martin, D. M. Guldi, *Chem. Soc. Rev.* **2005**, *34*, 31; k) L. Valentini, F. Mengoni, I. Armentano, J. M. Kenny, L. Ricco, M. J. Alongi, S. Trentini, M. A. Russo, *J. Appl. Phys.* **2006**, *99*, 114305/1; l) I. Robel, B. A. Bunker, P. V. Kamat, *Adv. Mater.* **2005**, *17*, 2458.
- [22] a) V. Georgakilas, K. Kordatos, M. Prato, D. M. Guldi, M. Holzinger, A. Hirsch, *J. Am. Chem. Soc.* **2002**, *124*, 760; b) H. Murakami, T. Nomura, N. Nakashima, *Chem. Phys. Lett.* **2003**, *378*, 481; c) D. M. Guldi, M. Marcaccio, D. Paolucci, F. Paolucci, N. Tagmatarchis, D. Tasis, E. Vazquez, M. Prato, *Angew. Chem.* **2003**, *115*, 4338; *Angew. Chem. Int. Ed.* **2003**, *42*, 4206; d) H. Li, B. Zhou, L. Gu, W. Wang, K. A. Shiral Fernando, S. Kumar, J. F. Allard, Y.-P. Sun, *J. Am. Chem. Soc.* **2004**, *126*, 1014; e) A. B. Artyukhin, O. Bakajin, P. Stroeve, A. Noy, *Langmuir* **2004**, *20*, 1442; f) J. Zhu, M. Yudasaka, M. F. Zhang, S. Iijima, *J. Phys. Chem. B* **2004**, *108*, 11317; g) D. M. Guldi, G. M. A. Rahman, N. Jux, D. Balbinot, N. Tagmatarchis, M. Prato, *Chem. Commun.* **2005**, 2038; h) G. M. A. Rahman, D. M. Guldi, E. Zamboni, L. Pasquato, N. Tagmatarchis, M. Prato, *Small* **2005**, *1*, 527; i) D. M. Guldi, G. M. A. Rahman, M. Prato, N. Jux, S. Qin, W. T. Ford, *Angew. Chem.* **2005**, *117*, 2051; *Angew. Chem. Int. Ed.* **2005**, *44*, 2015; j) M. Alvaro, C. Aprile, B. Ferrer, H. Garcia, *J. Am. Chem. Soc.* **2007**, *129*, 5647.
- [23] a) D. M. Guldi, G. M. A. Rahman, J. Ramey, M. Marcaccio, D. Paolucci, F. Paolucci, S. Qin, W. T. Ford, D. Balbinot, N. Jux, N. Tagmatarchis, M. Prato, *Chem. Commun.* **2004**, 2034; b) D. M. Guldi, G. M. A. Rahman, S. Qin, M. Tchoul, W. T. Ford, M. Marcaccio, D. Paolucci, F. Paolucci, S. Campidelli, M. Prato, *Chem. Eur. J.* **2006**, *12*, 2152; c) C. Ehli, S. Campidelli, F. G. Brunetti, M. Prato, D. M. Guldi, *J. Porphyrins Phthalocyanines* **2007**, *11*, 442; d) T. Umeyama, M. Fujita, N. Tezuka, N. Kadota, Y. Matano, K. Yoshida, S. Isoda, H. Imahori, *J. Phys. Chem. C* **2007**, *111*, 11484; e) F. Cheng, A. Adronov, *J. Porphyrins Phthalocyanines* **2007**, *11*, 198; f) D. Ren, Z. Guo, F. Du, J. Zheng, Y. Chen, *J. Nanosci. Nanotechnol.* **2007**, *7*, 1539.
- [24] a) D. M. Guldi, G. M. A. Rahman, N. Jux, D. Balbinot, U. Hartnagel, N. Tagmatarchis, M. Prato, *J. Am. Chem. Soc.* **2005**, *127*, 9830; b) G. M. A. Rahman, D. M. Guldi, R. Cagnoli, A. Mucci, L. Schenetti, L. Vaccari, M. Prato, *J. Am. Chem. Soc.* **2005**, *127*, 10051; c) D. M. Guldi, G. M. A. Rahman, V. Sgobba, N. A. Kotov, D. Bonifazi, M. Prato, *J. Am. Chem. Soc.* **2006**, *128*, 2315; d) C. Ehli, G. M. A. Rahman, N. Jux, D. Balbinot, D. M. Guldi, F. Paolucci, M. Marcaccio, D. Paolucci, M. Melle-Franco, F. Zerbetto, S. Campidelli, M. Prato, *J. Am. Chem. Soc.* **2006**, *128*, 11222; e) V. Sgobba, G. M. A. Rahman, D. M. Guldi, N. Jux, S. Campidelli, M. Prato, *Adv. Mater.* **2006**, *18*, 2264; f) S. Campidelli, C. Klumpp, A. Bianco, D. M. Guldi, M. Prato, *J. Phys. Org. Chem.* **2006**, *19*, 531.
- [25] a) D. M. Guldi, G. M. A. Rahman, F. Zerbetto, M. Prato, *Acc. Chem. Res.* **2005**, *38*, 871; b) D. M. Guldi, *Chem. Soc. Rev.* **2002**, *31*, 22; c) D. M. Guldi, G. M. A. Rahman, V. Sgobba, C. Ehli, *Chem. Soc. Rev.* **2006**, *35*, 471.
- [26] M. N. Tchoul, W. T. Ford, M. K. Gheith, J. P. Wicksted, M. Motamedi, *Polym. Prepr. (Am. Chem. Soc. Div. Polym. Chem.)* **2005**, *46(1)*, 222.
- [27] a) K. Saito, V. Troiani, H. Oiu, N. Solladie, T. Sakata, H. Mori, M. W. R. Ohama, S. Fukuzumi, *J. Phys. Chem. C* **2007**, *111*, 1194; b) Z. Gasyna, I. Browett, M. Stillman, *J. Inorg. Chem.* **1985**, *24*, 244; c) C. Inisan, J.-Y. Saillard, R. Guillard, A. Tabard, Y. L. Mest, *New J. Chem.* **1998**, *22*, 823.
- [28] a) S. Campidelli, C. Sooambar, E. Lozano-Diz, C. Ehli, D. M. Guldi, M. Prato, *J. Am. Chem. Soc.* **2006**, *128*, 12544; b) M. S. Strano, C. A. Dyke, M. L. Ursey, P. W. Barone, M. J. Allen, H. W. Shan, C. Kittrell, R. H. Hauge, J. M. Tour, R. E. Smalley, *Science* **2003**, *301*, 1519.
- [29] a) M. Alvaro, P. Atienzar, P. Cruz, J. L. Delgado, V. Troiani, H. Garcia, F. Langa, A. Palkar, L. Echegoyen, *J. Am. Chem. Soc.* **2006**, *128*, 6626; b) R. Chitta, A. S. D. Sandanayaka, A. L. Schumacher, L. D'Souza, Y. Araki, O. Ito, F. D'Souza, *J. Phys. Chem. C* **2007**, *111*, 6947.
- [30] a) C. Luo, D. M. Guldi, M. Maggini, E. Menna, S. Mondini, N. A. Kotov, M. Prato, *Angew. Chem.* **2000**, *112*, 4052; *Angew. Chem. Int. Ed.* **2000**, *39*, 3905; *Angew. Chem. Int. Ed.* **2000**, *39*, 3905; b) D. M. Guldi, C. Luo, D. Koktysh, N. A. Kotov, T. Da Ros, S. Bosi, M. Prato, *Nano Lett.* **2002**, *2*, 775; c) D. M. Guldi, F. Pellarini, M. Prato, C. Granito, L. Troisi, *Nano Lett.* **2002**, *2*, 965; d) D. M. Guldi, I. Zilbermann, A. Lin, M. Braun, A. Hirsch, *Chem. Commun.* **2004**, 96; e) D. M. Guldi, N. A. Kotov, A. Hirsch, M. Prato, *J. Phys. Chem. B* **2004**, *108*, 8770.
- [31] For the deposition of SWNT-PVBTA<sup>n+</sup> onto the polycationic PDDA one may expect repulsion. However, we obtained an even more uniform SWNT film on PDDA than on polyanionic polystyrene sulfonate (PSS<sup>-</sup>). This may be attributable to the strong hydrophobic interactions between the positively charged polymers that may overcome the electrostatic repulsions, which are, however, only effective if the ion pairs are truly separated. Interestingly, the above-mentioned octacationic porphyrins are also rather hydrophobic as they dissolve easily in chlorinated hydrocarbons.
- [32] M. Zhang, L. Su, L. Mao, *Carbon* **2006**, *44*, 276.

Received: May 27, 2008  
Published online: September 2, 2008